TUDelft

Delft University of Technology

Impedance Standard Substrate Characterization and em model definition for Cryogenic and Quantum-Computing Applications

Shokrolahzade, Ehsan; Sebastiano, Fabio; Mubarak, Faisal; Babaie, Masoud; Spirito, Marco

Important note
To cite this publication, please use the final published version (if applicable).
Please check the document version above.

Impedance Standard Substrate Characterization and EM model definition for Cryogenic and Quantum-Computing Applications

Ehsan Shokrolahzade[1], Fabio Sebastiano[2], Faisal Mubarak[3], Masoud Babaie[1], Marco Spirito[1]

[1]Electronic Circuits and Architectures (ELCA), TU Delft, The Netherlands
[2]Department of Quantum & Computing Engineering & QuTech , TU Delft, The Netherlands
[3]VSL, Dutch Metrology Institute, The Netherlands

Abstract—**In this contribution, we describe the modeling approaches and the characterization procedures used to develop accurate standard models for cryogenic, probe-level, calibrations substrates.**

The key electrical and mechanical parameters of the impedance terminations and the lines used in commercially available impedance standard substrates are first characterized versus temperature. After, these component are simulated using 2.5D EM solvers including their mechanical variation when exposed to cryogenic temperatures, to extract their nominal response at 7 Kelvin. The quality of the resulting calibrations at cryogenic is evaluated first using independent CPW lines on the calibration substrates and then by measuring the response of a transformer-based resonator realized on a Si-based technology.

Ambient temperature models are used as a comparison, to highlight the accuracy improvement that can be achieved employing optimized Cryo-EM based models.

I. INTRODUCTION

Cryogenic electronics have historically played a crucial role in metrology, high-energy physics experiments and astronomical instrumentations. In recent years, a growing demand for solid-state circuits operating at cryogenic temperatures is coming from space-borne and quantum-computing applications. The need for higher production volumes and higher complexity has also triggered a shift in the adopted technology platforms to one that would support larger fabrication volumes and higher integration with lower unit cost, i.e., cryo-CMOS. Following the same development path in knowledge and performance used for integrated circuits at ambient temperatures, also cryo-CMOS proponents are investing in improving the technology models for both DC and high-frequency response. In this validation/optimization process, on-wafer, probe-level measurements are a viable approach that reduces the efforts required for de-embedding in comparison to typical setups employing liquid Helium cooling, e.g., discrete dipstick setups [1].

For high-frequency device characterization, the calibration process sets the acquisition accuracy, while, in turn, the knowledge of the standards used in the calibration process sets the calibration accuracy to a first degree. Prior work on on-wafer cryogenic calibration has first focused on the time stability [2] [3], as these systems are more sensitive than their room-temperature counterparts, and later on the definition of the standards response at cryogenic temperatures [4][5]. The cryogenic response of the calibration devices was derived by extracting the propagation constant of the different lines used

for TRL calibrations and the low-frequency capacitance per unit length as described in [6], thus confining the accuracy of the extraction approach to the frequency range where TRL is accurate, i.e., when the excess phase delay of the line exceeds the thru delay by 20°. Nevertheless, when targeting model extraction and verification, broadband calibration techniques, i.e., employing broadband loads, are often preferred. Despite this, the knowledge of the lumped standards used in these calibrations, i.e., open, load, short, and thru, in commercially available substrates [7] is only provided at room temperature with information of the linear temperature dependence, only of DC value of the load standard. To improve the accuracy of the standard definitions, and thus, in turn of the probe level calibration, this work described the procedures for the extraction, as a function of temperature, of the electrical parameters of the conductive and dielectric layers composing two commercially available impedance standard substrates (i.e., Alumina-based and Quartz-based). Furthermore, the mechanical shrinkage due to the temperature change from room temperature to cryogenic one is derived, and the method of [8] and [9] is employed to define the frequency-dependent response of the artifacts used in the calibration procedure.

II. MEASUREMENT SETUP

The employed on-wafer cryogenic setup is shown in Fig. 1. The setup comprises an R&S ZNB40 vector network analyser (VNA) and a Lakeshore CPX cryogenic probe station (see Fig. 1), employing 100um GSG Picoprobes.
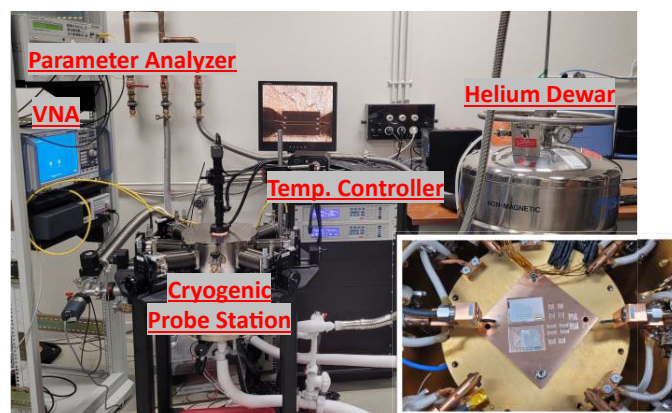

Fig. 1: Cryogenic probe station measurement setup, (inset) copper plate for ISS inserts.

The dies were mounted with conductive glue on a copper plate (CP) in the vacuum chamber to ensure proper thermalization, as shown in the inset of Fig. 1. In addition, a Keysight E5270B parameter analyser is employed for DC measurements.

III. IMPEDANCE STANDARD SUBSTRATES

For the calibration analysis described in this paper, two impedance standard substrates (ISS) were selected, one based on gold lines on an Alumina carrier [10] and one employing Aluminum lines on a Quartz substrate [11].

The lateral dimensions of the structures present on the two ISS, were extracted at ambient temperature using a laser scanning microscope Keyence VK-X250 while the height of the structures was measured on a few cross sections using a Veeco Dektak 8 stylus profiler.

Since the conductive layers are deposited as a thin film on the dielectric substrate (carrier) during fabrication, it is assumed in this paper that the thermal expansion coefficient will be defined by the carrier material.

In order to compute the dimension of the structures at cryogenic temperature, the thermal expansion coefficients of the two materials are extracted from [12] and [13], for the Alumina and Quartz case, respectively, and are summarized in Table 1.

Table 1: Thermal expansion coefficient and electrical parameters of the ISS materials considered in this work.

Material	Thermal contraction $(\Delta L/L_0)$ (293K to 4K)	Relative electrical permittivity	Loss tangent(tan δ)
Alumina	0.063%	9.9	1e-4
Fused Quartz	0.015%	3.81	4e-4

Given the extreme purity of the dielectric material used to realize both ISSs, the permittivity and loss tangent of these dielectrics are assumed constant over the considered temperature range at the value shown in Table 1.

The resistivity of the conductive layers, being strongly dependent on the technology process used and their metal concentrations, were extracted in-situ at different temperatures, see Fig. 2, to realize the reference data for the models described in the next section.
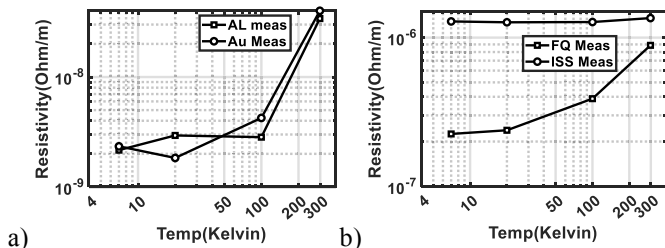
Fig. 2: Measured resistivity of metal layers in Alumina and Quartz ISS, a) conductive layers (i.e., gold and aluminium), b) resistive layers.

IV. EM MODEL GENERATION

The mechanical and electrical properties of the structures were characterized versus temperature, as described in section III and used to realize electro-magnetic (EM) models, see Fig. 3, to generate the standard response at cryogenic temperatures, i.e., 7K.

Fig. 3: Quartz ISS used for Cryo-EM model extractions.

Employing EM-generated models from the calibration standards provides the advantage of realizing probe maker independent calibration definitions as was demonstrated in [13] (note that the probe pitch is still mapped in the EM generated models), and allows to easily employ a parametric variation on the material responses to easily account for process fabrication spread. As an example, given the larger change of the resistivity of the resistor material employed in the Quartz technology (see Fig. 2 b), a parametric simulation of the load standard for a range of layer resistivity values was carried out, see Fig. 4.
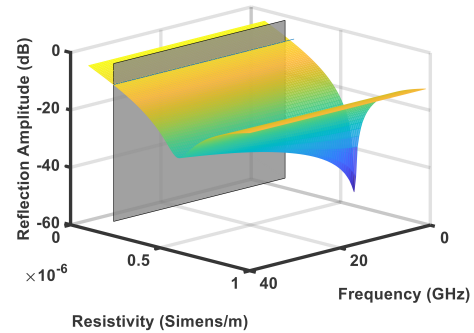
Fig. 4: Frequency response of Quartz ISS load versus material resistivity extracted from parametric EM simulation.

This over-determined look-up table for the standard response allows, at measurement time, by performing a simple DC measurement of the load, to identify the most accurate frequency response for that component, as shown in Fig. 4 grey plane.

V. CALIBRATION VALIDATION

The proposed EM models were first tested at ambient temperature to evaluate the measurement quality of the setup. The calibration routine used in the rest of the paper is the SOLR, but similar consideration can be derived when applying it to an LRM algorithm.

To quantify the quality of a calibration, we use the worst-case bound metric, defined as shown in eq. 1.

$$WCB(f) = \max \left| S'_{ij}(f) - S_{ij}(f) \right| \qquad (1)$$

Where S' is the reference scattering matrix of a verification line (i.e., EM simulated S-parameters), S(f) is the frequency dependent scattering matrix resulting from the investigated calibrations and $i, j \in [1,2]$.
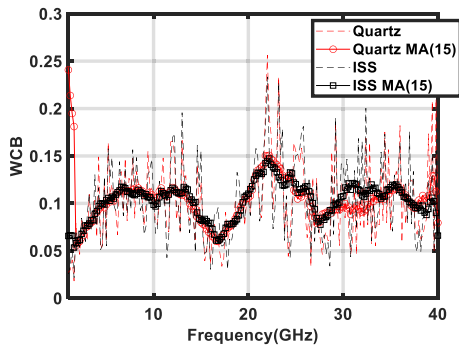
Fig. 5: Calibration quality evaluated using the WCB metric, for Alumina and Quartz ISS substrates at ambient temperature: (dashed) measured data, (solid with marker) employing a moving average (MA) of 15 to remove random effect due to mechanical vibration.

Two major effects limiting the accuracy were identified, first the mechanical coupling of the setup to the vibration of the environment (i.e., absence of vibration isolation) resulted in "noisy" traces. A second effect, as was identified in [2], is that microwave probes provide significantly more damage when operating in vacuum at low temperatures, resulting in larger contact resistance variations across different landings. To highlight the random nature of this effect, the data are presented as extracted from the measurement (dashed) and using a moving average (across frequency) of 15 (solid with symbol), as shown in Fig. 5.

As was shown in Fig. 2 b),the resistivity of the layer used for the match termination might vary considerably from room temperature (RT) to the cryogenic environment. This depends strongly on the technology used and can result in potential large variations even within the same technology. To compensate for this effect, the parametric approach shown in Fig. 4 can be employed. To experimentally demonstrate this, an 1320 um CPW located on the Quartz substrate was measured at 7K.
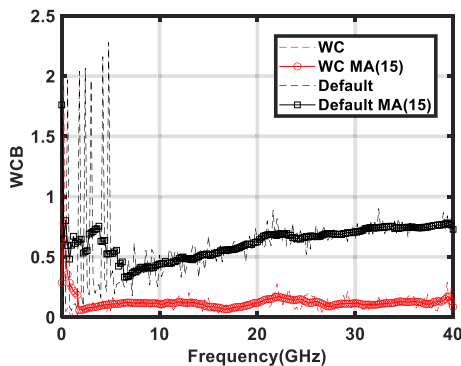

Fig. 6: WCB plot of a 1320 micron CPW on Quartz substrate using: (Default) calibration set employing default Cryo parameter response (i.e., nominal conductivity) and (WC) load response matching the measured device DC resistivity.

All the standards used for the calibration process were acquired at the same cryogenic temperature as the DUT. The corrections were performed first using the Cryo-EM calibration kit definitions (black line) and after (on the same raw data) applying the load compensation technique using a conductivity of 4.55e-6 S/m as shown in Fig. 4 (grey plane). Fig. 6 shows

the WCB metric for this test highlighting the importance of the proper load value in lumped calibration kit definitions. Furthermore, as was discussed in the previous sections, using EM-based models allows to accurately map the changes in mechanical and electrical response at cryogenic temperature in the model definitions.

a)   b)
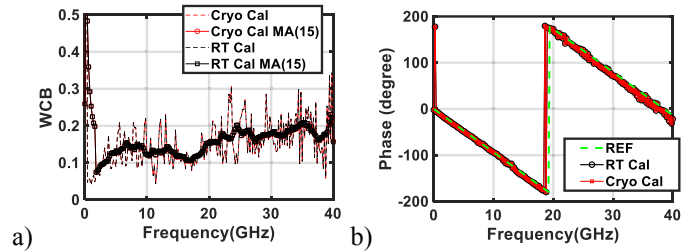
Fig. 7: WCB of CPW line on an Alumina substrate measured at 7K using calibration definition for the standards derived from RT response (RT – black line) and from cryogenic temperature responses (Cryo Cal – red line).

To evaluate the impact of this, a 3500 um CPW line was measured at cryogenic temperature (i.e., 7K) on an Alumina substrate, with the required standards to perform an SOLR calibration routine. EM models of the standards are extracted at room and cryogenic temperatures, to allow probe independent definitions, as discussed in Section IV. While the Short and Open definitions vary up to -45dB in the higher frequency range (vector difference of the reflection coefficient), the low conductivity variation of the resistive layer confines the load variation to below -50dB. This reduced variation of the load standard (when compared to the fused quartz substrate) minimizes the calibration quality impact as can be seen in Fig. 7 a).

The accurate phase alignment of both calibrations with the reference data of the 3500 um CPW line indicate a correct placement of the calibration reference planes.

VI. DUT MEASUREMENTS

To validate that Cryo-EM models will enable to realize accurate, probe-substrate independent calibration definitions, an independent device, namely a transformer-based resonator (shown in Fig. 8), realized in TSMC 40-nm bulk CMOS was measured. The same raw data were corrected using the calibrations derived using both ISS substrates and compared to the device response model.
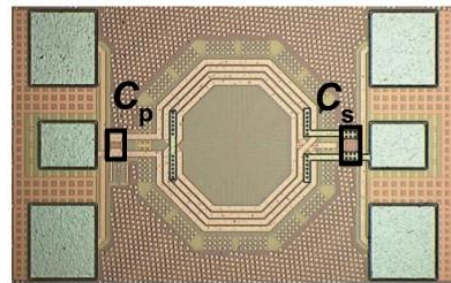

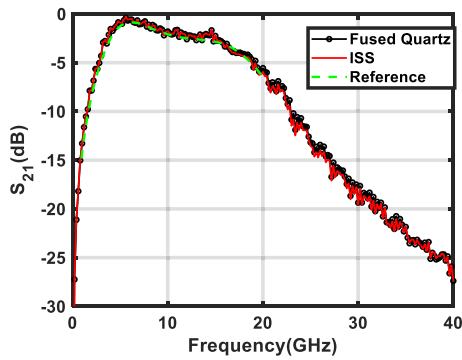Fig. 8: Microphotograph of transformer-based resonator realized in TSMC 40-nm bulk CMOS [14].

Fig. 9: Comparison of the S_{21} parameter of the resonator corrected using calibration realized employing Cryo-EM model on both Alumina and Quartz ISS (black and red trace, respectively) and resonator model response (only available in the 0.2-20GHz range from [14]).

The device was measured together with the standards on both ISS substrates at 7K.

Fig. 9 presents the corrected data employing both the Quartz and Alumina calibration using Cryo-EM models. A very good agreement is achieved between the two calibrations and with the reference data.
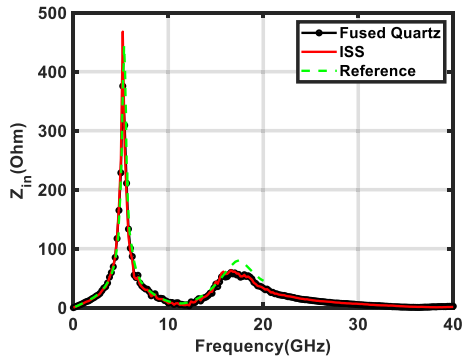

Fig. 10: Comparison of the input impedance of resonator (Zin) corrected using calibration realized employing Cryo-EM model on both Alumina and Quartz ISS (black and red trace, respectively) and resonator model response (only available in the 0.2-20GHz range from [14]).

Fig. 10 presents the input impedance of the resonator, where the resonance peak is clearly present, and the good agreement between both calibrations employing Cryo-EM data with the model substantiates the claim of accurate probe-independent calibration models.

VII. CONCLUSION

In this paper, we applied the concept of EM-based calibration standard definition to cryogenic environments. First, the electrical parameters of the materials that are part of the structures employed in the calibration process were extracted versus temperature and their mechanical variation due to thermal compression was considered. Then, the approach of load variation compensation using an over-determined EM simulation and a DC in-situ (cryogenic) measurement was described. Moreover, several comparative analysis at cryogenic temperatures (7K) were presented, employing both ISS considered in this work highlighting the quality and consistency of the achieved cryogenic calibration using the proposed EM approach. Finally, an independent DUT realized in a Silicon-based CMOS process was employed as a reference device to highlight the capability of providing probe-substrate independent definition using the Cryo-EM approach.

REFERENCES

[1] P. A. 'T Hart, M. Babaie, E. Charbon, A. Vladimirescu and F. Sebastiano, "Characterization and Modeling of Mismatch in Cryo-CMOS," in IEEE Journal of the Electron Devices Society, vol. 8, pp. 263-273, 2020.

[2] V.M. Hietala, M.S. Housel, R.B. Caldwell, "Network Analyzer Calibration for Cryogenic On-Wafer Measurements", 43rd ARFTG Conference Digest, May 1994.

[3] J. Laskar, J.J. Bautista, M. Nishimoto, M. Hamai, and R. Lai, "Development of Accurate On-wafer, Cryogenic Characterization Techniques", IEEE Trans. Microwave Theory and Tech., vol. 44, no. 7, pp. 1178–1183, July 1996.

[4] Rumiantsev, R. Doerner and P. Sakalas, "Verification of wafer-level calibration accuracy at cryogenic temperatures," 2006 68th ARFTG Conference: Microwave Measurement, 2006, pp. 1-4

[5] S. Boaventura et al., "Microwave Modeling and Characterization of Superconductive Circuits for Quantum Voltage Standard Applications at 4 K," in IEEE Transactions on Applied Superconductivity, vol. 30, no. 2, pp. 1-7, March 2020

[6] R. Marks, D. Williams, "Characteristic Impedance Determination Using Propagation Constant Measurements", IEEE Microwave and Guided Wave Lett., vol. 1, pp. 141–143, June 1991.

[7] CSR-8 Calibration Substrate Quick Reference Guide, website, 3/12/2022. [Online]. Available: https://www.formfactor.com/product/probes/calibration-tools-probes/csr-cal-substrates/#downloads

[8] E. Shokrolahzade, C. De Martino and M. Spirito, "Reduced Calibration Error Employing parametrized EM models and DC Load Extraction," 2023 100th ARFTG Microwave Measurement Conference, 2023,pp. 1-4

[9] M. Spirito, L. Galatro, G. Lorito, T. Zoumpoulidis and F. Mubarak, "Improved RSOL planar calibration via EM modelling and reduced spread resistive layers," 2015 86th ARFTG Microwave Measurement Conference, 2015, pp. 1-5

[10] 101-190C Impedance Standard Substrate Map, website, 3/12/2022. [Online]. Available: https://www.formfactor.com/download/iss-map-101-90/?wpdmdl=3159

[11] Fused silica calkits (fss), website, 3/12/2022. [Online]. Available: https://vertigo-tech.com/services/fused-silica-calkits-fss/

[12] Zhipeng Xie, Weijiang Xue, Haibo Chen, Yong Huang, "Mechanical and thermal properties of 99% and 92% Alumina at cryogenic temperatures," Ceramics International, Volume 37, Issue 7, 2011. Quartz Wafer, website, 3/12/2022. [Online]. Available: https://planoptik.com/products/glass-wafer/

[13] L. Galatro, F. Mubarak and M. Spirito, "On the definition of reference planes in probe-level calibrations," 2016 87th ARFTG Microwave Measurement Conference (ARFTG), 2016, pp. 1-4.

[14] B. Patra, M. Mehrpoo, A. Ruffino, F. Sebastiano, E. Charbon and M. Babaie, "Characterization and Analysis of On-Chip Microwave Passive Components at Cryogenic Temperatures," in IEEE Journal of the Electron Devices Society, vol. 8, pp. 448-456, 2020